Control of the Permeability of a Porous Media Using a Thermally Sensitive Polymer

Alexis Tran-Viet, Alexander F. Routh, and Andrew W. Woods
BP Institute for Multiphase Flow, University of Cambridge, Cambridge CB3 OEZ U.K.

DOI 10.1002/aic.14352
Published online January 20, 2014 in Wiley Online Library (wileyonlinelibrary.com)

Experiments explore the reduction in permeability of a porous bead pack when a suspension of thermally responsive polymer is injected and the temperature then increased above the thermal activation temperature. The change in permeability is greater with higher polymer concentration, provided that the ionic concentration of the solution is sufficient for floc formation. The time for activation of the blocking effect is within tens of seconds to minutes of when the polymer solution is heated. This is consistent with the timescale for diffusion-limited aggregation, although the detailed value depends on the geometry and polymer concentration. Dynamical experiments demonstrate that once the porous media is blocked, adding additional polymer has no effect. The mechanism for permeability reduction may be modeled in the context of a pore-network model, and we build a simple model to illustrate the permeability reduction as a function of the fraction of pores links which are blocked. © 2014 American Institute of Chemical Engineers *AIChE J*, 60: 1193–1201, 2014

Keywords: porous media, colloids, complex fluids

Introduction

During water injection to displace oil through a permeable reservoir, the flow selects high-permeability channels and thereby bypasses much of the fluid trapped in lower permeability regions of the reservoir. Polymers are sometimes used to enhance the secondary and tertiary recovery of oil by blocking high permeability channels, so that injection of more water into the reservoir promotes displacement of the oil from lower permeability regions of rock. Often viscosifying agents such as polyacrylamide and xantham gum are used, but these materials have a set rheology as a function of concentration and it is not always possible to control the region of the reservoir blocked by the polymers.[1]

Flow in porous media has been extensively studied.[2] Viscous fingering, where a less viscous fluid displaces a more viscous one through fingers rather than a planer front, has been observed and modeled for heterogeneous[3] and homogeneous[4] permeability fields.

Recently, there has been considerable interest in the use of responsive materials which may provide more control on the location where such polymers act within the reservoir. Ideally, the polymer floods the high permeability zones, and then viscosifies, so as to impede further flow through these regions. One strategy for controlling the activation of the polymer is to use a thermally responsive polymer, so that during injection, with cold water, the polymer remains cold and mobile. However, as the injected fluid migrates into the reservoir, it warms up and the polymer solution either viscosifies, or the polymer drops out of solution and blocks the flow.

One such responsive polymer is poly(N-isopropylacrylamide) (PNIPAM). Below 32°C water is a good solvent for the polymer which will be in an extended state. Above 32°C water is a bad solvent and the polymer chains collapse in size as the chains attempt to minimize polymer solvent interactions.[5] In addition, pH, ionic strength, and pressure can affect the critical behavior of PNIPAM.[6] Extensive work has been carried out using PNIPAM crosslinked with methylene bisacrylamide to make particles.[7] These microgel particles swell at low temperatures and hence behave as smart particles that can be used for a range of purposes such as delivery devices or rheological control agents. Once PNIPAM chains collapse they may aggregate, with other chains, as determined by the colloidal stability of the polymer which, in turn, is controlled by the level of charge associated with initiator moieties. Any background electrolyte will screen the stabilizing charge so that above a critical salt concentration, the polymer chains will aggregate into larger flocs.

The purpose of this work is to explore the impact of the rheological control associated with temperature changes on the permeability of a porous layer. We first report some novel experiments in which a bead pack is flooded with a cold polymer laden solution and then heated for a given period of time, comparing the permeability before and after heating. Then we look at the effect of flowing cold polymer solutions into a bead pack, with a specified temperature field imposed on it. Finally, we build a phenomenological model, based on the idea that aggregates can block pore throats, to rationalize our observations.

Materials and Methods

PNIPAM powder with a molecular weight of 3×10^5 g/mol was purchased from Scientific Polymer Products. Solutions were

Correspodence concerning this article should be addressed to A.F. Routh at afr10@cam.ac.uk.

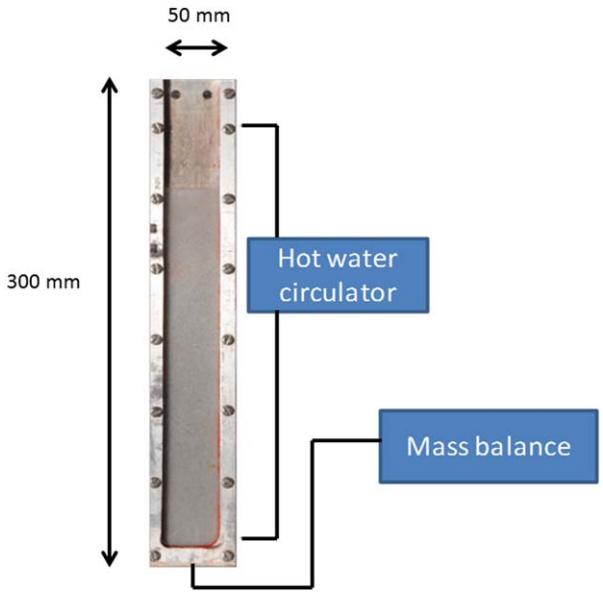

Figure 1. Front view of the experimental setup. The tank is 30 cm long, 5 cm wide, and 0.2 cm thick.

[Color figure can be viewed in the online issue, which is available at wileyonlinelibrary.com.]

made up in deionized water and sodium chloride was then added to achieve a desired electrolyte concentration. It was found that solutions were stable over a 1 week period and all samples were used within this time-frame.

The flow tank had dimensions 300 mm in height, 50 mm width, and 2 mm thickness and was constructed from a milled piece of aluminium which constituted the back and sidewalls of the cell, whereas the front of the cell was composed of a plate of Perspex of 2 mm thickness. Three cavities at the back of the aluminium block were connected to water circulator units. A picture of the tank can be seen in Figure 1. Since the aluminium has high thermal conductivity and the bead pack was only 2 mm thick, the heating of the flow domain to the desired temperature occurs within seconds. We used beads of diameter 0.5 mm for which the flow was controlled according to Darcy's law.

Experiments where the tank is preloaded with polymer

Cold polymer solution is injected and heated above the lower critical solution temperature. After precipitation, the permeability was measured by flowing water of the same ionic strength and temperature and measuring the flow rate. The flow was driven by gravity with a known head between the free surface and the outlet pipe, so the effective permeability of the cell could be inferred from the measured flow rate. A small piece of sponge prevented the glass ballotini from flowing out of the tank. Calibration experiments demonstrated that pressure losses in the outlet tubing, and across the sponge, were negligible compared to those in the bead pack itself. Additionally, there is no evidence that flow, or heating, induced structural changes in the bead pack during the experiments.

Experiments where polymer is flowed into the tank

A steep temperature gradient is set in the tank by connecting the two bottom chambers to a hot water circulator, and the top chamber to a cold refrigeration circulator. The temperature of the bead pack changed from 20 to 45°C over a distance of 10 mm. The temperature is measured using thermochromic liquid crystal sheets from LCR Hallcrest.

The PNIPAM fronts or slugs of concentrations between 0.625 and 7.5 g/L are injected from the top of the tank and flow by a gravity drain. The head pressure is varied by changing the difference in height of the fluid level in the tank and of the outlet pipe and is quoted as a head pressure of a water column, for example, 10 cm H_2O is equivalent to a pressure difference 981 Pa. Additionally, the PNIPAM solution was occasionally dyed with fluorescein to track the fluid front visually. The flow rate was measured with a mass balance.

Figure 2 shows the experimental setup during an experiment. As the PNIPAM heats up in the bead pack it precipitates. The opaque region in Figure 2 is a precipitated PNIPAM layer and it is 11 mm thick and located just below the temperature front. The temperature is measured using the liquid crystal strips and these are located on the outside of the tank. It is simple to balance the heat flow by conduction through the aluminium tank with a convective heat-flow in the liquid stream. Doing so indicates that for flow rates below 9.6×10^{-3} g/s the temperature field may be taken as stationary.

Results

Experiments where the tank is preloaded with polymer

Effect of PNIPAM Concentration and Heating Time. In each experiment, the cell was flooded with a cold PNIPAM solution of known concentration. The tank was then heated

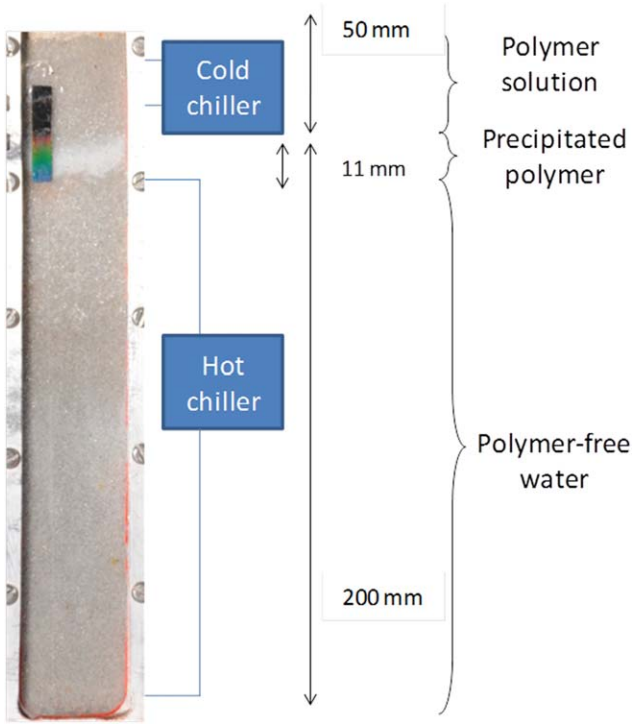

Figure 2. Injection experiments of a PNIPAM front (2.5 g/L) into a frozen temperature field.

NB: The temperature is measured outside of the bead pack, however, at small flow rates thermal equilibrium is achieved between the bead pack and the Perspex wall. [Color figure can be viewed in the online issue, which is available at wileyonlinelibrary.com.]

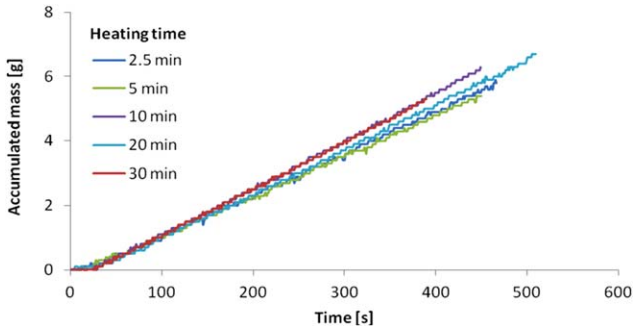

Figure 3. Accumulated mass as a function of time for 7.5 g/L PNIPAM solution.

The solutions were heated to 45°C for different times and a head pressure of 30 cm H_2O applied. [Color figure can be viewed in the online issue, which is available at wileyonlinelibrary.com.]

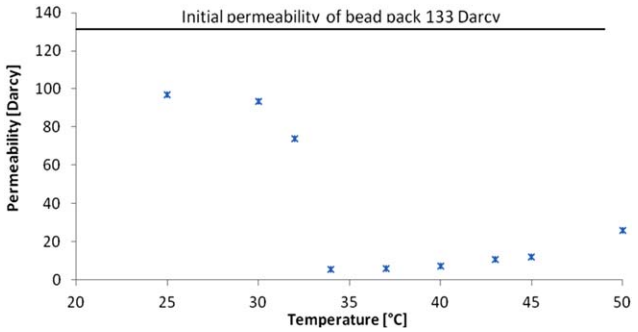

Figure 5. Permeability of precipitated PNIPAM solution (7.5 g/L) in a bead pack as a function of temperature.

The applied head is 30 cm, the heating time is 5 min, and the electrolyte concentration is 50 mM. [Color figure can be viewed in the online issue, which is available at wileyonlinelibrary.com.]

for a certain amount of time and subsequently the effective permeability was measured, based on the applied head and flow speed, assuming a uniform flow. Five different PNIPAM concentrations between 0.625 and 10 g/L and five heating times ranging from 2.5 to 30 min were investigated. In all the experiments, we found the mass flowing through the cell increased linearly with time, suggesting a constant flow rate (Figure 3). For each concentration, the permeability measured in the cell is essentially independent of the heating time, provided the heating is in excess of a few minutes, as summarized in Figure 4. The permeability decreases with increasing PNIPAM concentration. This may be associated with the increased aggregation of PNIPAM precipitates, leading to the blocking of more of the flow paths. At the higher polymer concentrations, the permeability may even become controlled by flow through an entangled polymer network in the pores and pore throats.

Temperature Dependence. The permeability was measured as a function of temperature, while fixing the PNIPAM concentration (7.5 g/L), heating time (5 min), and concentration of sodium chloride (50 mM). The highest temperature investigated was 50°C and the results are shown in Figure 5. For temperatures below the 32°C, it was visually observed that the cloudy PNIPAM solution was washed out of the cell. However, the measured permeability of 97 Darcy is below that of the fresh bead pack, 133 Darcy. This might be due to adsorption of some PNIPAM molecules to the beads, the Perspex cell wall, or the aluminium block. Alternatively the lower permeability may be due to precipitation of some of the PNIPAM, even at lower temperatures. For temperatures above 32°C, the permeability drops drastically to a minimum value of 5.5 Darcy at 34°C, and then recovers to 26 Darcy at 50°C. The drop in permeability above 32°C is caused by the phase transition of PNIPAM and precipitation of the polymer out of solution. As the temperature is increased further, the permeability increases. A possible explanation is that the polymer chains collapse further at higher temperature and hence some of the pore throats become more permeable to flow. This is supported by the data from Morris et al.,[8] who show PNIPAM microgel particles continuing to reduce in size as the temperature was raised to 80°C.

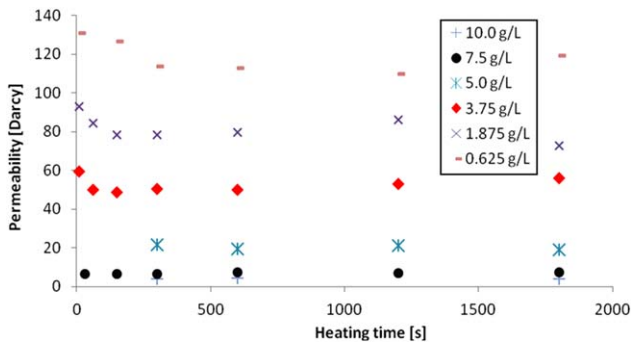

Figure 4. Permeability of a fully saturated PNIPAM bead pack at 45°C for different concentrations and heating times.

[Color figure can be viewed in the online issue, which is available at wileyonlinelibrary.com.]

Ionic Strength Dependence. The permeability of a bead pack with 7.5 g/L PNIPAM solution for a heating time of 5 min at 45°C was measured for different sodium chloride concentrations up to 50 mM, with the results shown in Figure 6. The use of very pure deionized water with a conductivity of 5.5 μS m^{-1}, achieves a permeability of about 40 Darcy. This was sustained even after several pore volumes of water were flooded through the cell. Increasing the NaCl concentration to between 0.02 and 0.05 mM led to an increase in the permeability to about 90 Darcy. Higher salinities led to a dramatic reduction in permeability to a value of around 6 Darcy at 0.2 mM. It is likely that with sodium chloride concentrations above 0.1 mM, the PNIPAM

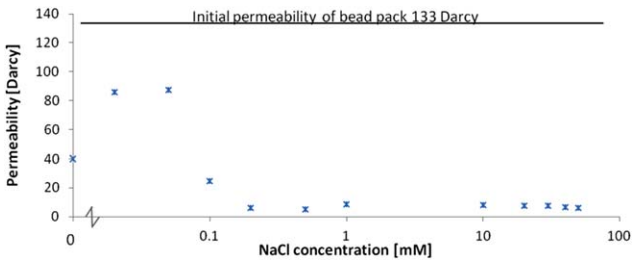

Figure 6. Permeability of precipitated PNIPAM solution (7.5 g/L) in a bead pack using a temperature of 45°C and a heating time of 5 min.

[Color figure can be viewed in the online issue, which is available at wileyonlinelibrary.com.]

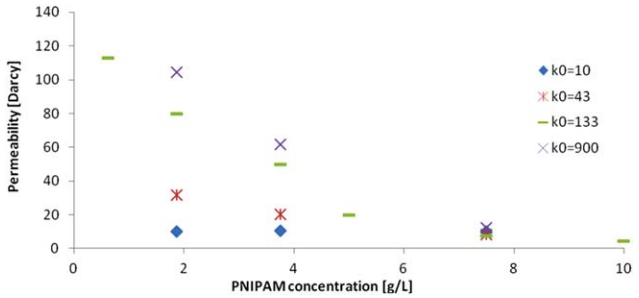

Figure 7. Final permeability for different PNIPAM concentration and four different initial permeabilites.

The electrolyte concentration is 50 mM NaCl, the temperature is 45°C, and the heating time is 5 min. [Color figure can be viewed in the online issue, which is available at wileyonlinelibrary.com.]

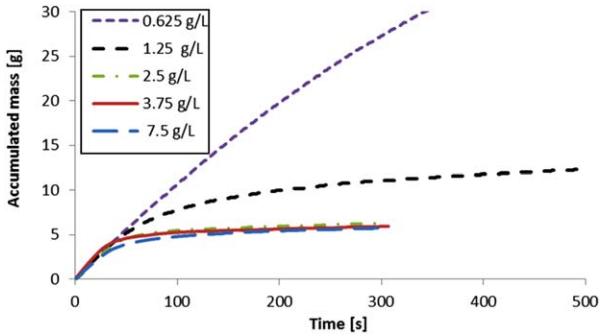

Figure 8. Accumulated mass as a function of time of a polymer front injected into a bead pack for 30 cm H_2O head pressure.

[Color figure can be viewed in the online issue, which is available at wileyonlinelibrary.com.]

particles aggregate and create flocs which block the flow paths. A possible explanation for the lowest salinity water giving a lower reading for permeability is that the double layer of deionized water is relatively large and this increases the effective particle size, reducing the pore sizes accordingly.

Initial Bead Size. One experiment was repeated using four different sizes of glass ballotini with a range of initial permeabilities. The results are shown in Figure 7. For a high PNIPAM concentration (7.5 g/L) the permeability drops to about 7 Darcy, regardless of the initial permeability of the bead pack. The likely reason is that once the polymer precipitates and blocks the pore throats, the effective permeability is controlled by the resistance to flow through the polymer network within the pore throats, provided this is much smaller than the original permeability associated with the bead pack.

Experiments where polymer is flowed into the tank

The polymer solution, at room temperature (20°C) is flowed into the warmed tank, under a fixed pressure head, and the flow rate in measured. The results are shown in Figure 8 for various concentrations of polymer. As expected the flow rate drops as the concentration is increased, but above a certain concentration, here 2.5 g/L, there is no benefit in increasing the polymer concentration further. Differentiating the data in Figure 8 one may obtain the permeability and this is shown in Figure 9, as a function of the amount of polymer added to the tank. The pleasing result is that using lower concentrations of polymer allows one to achieve the permeability reduction with a lower total amount of polymer. This effect is seen for two separate applied pressure heads.

The effect of the flow on the applied temperature field is investigated in Figures 10 and 11. Figure 10 shows the effect of flowing PNIPAM solution, at concentration 7.5 g/L, under a fixed pressure head of 30 cm H_2O. The temperature field is seen to distort slightly because of the introduction of cold polymer solution and the growth in the precipitated polymer region is also seen as the white precipitate. The solidified polymer region grows in size as the experiment proceeds and presumably provides a growing resistance to flow. This is also seen in Figure 11, which corresponds to the same experiment, but with an applied pressure head of 10 cm H_2O. Here the distortion to the temperature field is smaller, but again the growth of precipitated region is seen.

Effect of slug sizes

Instead of flowing a continuous stream of polymer, the effect of flowing slugs, preceded and followed by flows of water, was investigated. Figure 12 shows the accumulated mass when a fixed amount of PNIPAM was flowed into the tank, but the concentration and consequently slug volume were varied. The important result is the final slope of the curves in Figure 12, which correspond to the final permeability. The results are summarized in Figure 13 for two different amounts of PNIPAM. It can be seen that large volumes slugs, of dilute polymer, cause a larger drop in permeability.

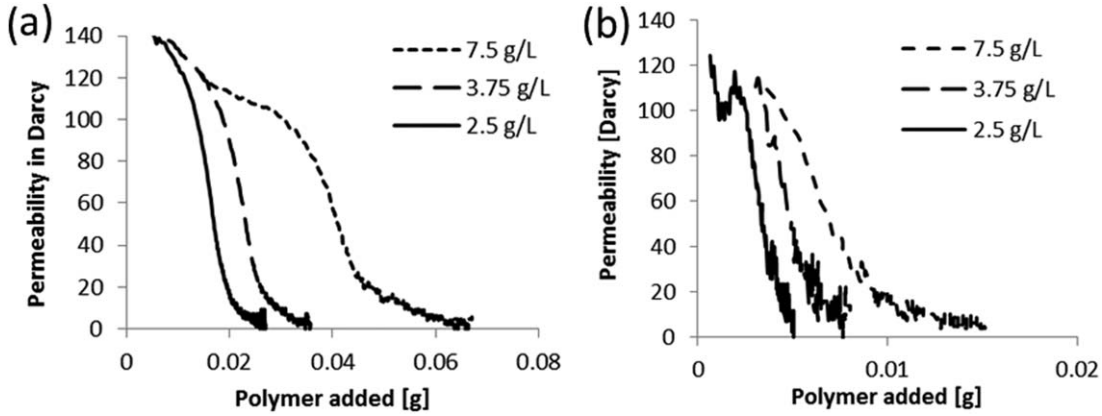

Figure 9. Permeability as a function of polymer added for (a) 30 cm H_2O head pressure and (b) 10 cm H_2O head pressure.

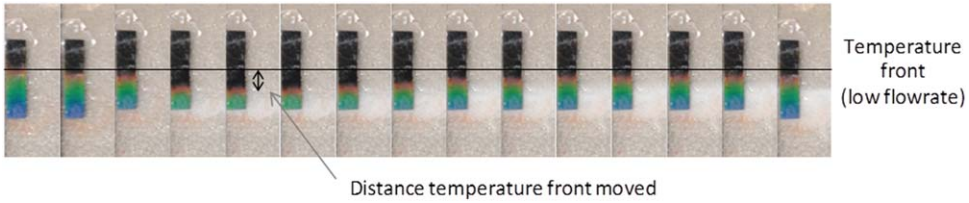

Figure 10. Experiments for the injection of PNIPAM front (7.5 g/L) into a static temperature field, pictures are taken every 5 s, the last two pictures are 60 s apart; arrow indicates 3 mm distance by which the temperature field has moved (30 cm H_2O head).

The color of the thermochromic strips indicates the temperature. Black indicates a temperature below 30°C, red a temperature above 30°C, green above 31°C, and blue above 35°C. [Color figure can be viewed in the online issue, which is available at wileyonlinelibrary.com.]

Model for Permeability Reduction

As indicated in the description of the experimental results, the reduction in permeability arises from the precipitation of the polymer and the subsequent aggregation into flocs, which are as large as the pore throats, and therefore impose a resistance on the flow. The flocs themselves are likely to be permeable and once sufficient pore throats are blocked, they control the effective permeability of the system. To explore this process, we can draw from literature on the growth of flocs from PNIPAM precipitates, and on the subsequent blocking of the porous system, modeled as a network of pores and throats.

The PNIPAM precipitates can aggregate provided that the ionic strength of the solution is greater than a few millimolar of sodium chloride, so that the aggregates are not stabilised by repulsive electrostatic forces.[9] When considering the PNIPAM precipitates aggregating, it is possible to imagine them initially precipitating, aggregating, and the flocs even subsequently breaking. This leads into a population balance equation for the distribution of floc sizes. Such a problem has been examined by Hounslow et al.[10,11] In this work, we prefer to take the simplified approach that only considers preformed base particles. These base particles, and the growing flocs, are free to diffuse in solution and upon contact with other flocs will aggregate. As the aggregation forms strong bonds between individual PNIPAM particles, it is usual to model the process as one of diffusion limited aggregation.[12,13] In an unconfined geometry, these aggregates are fractal and their compactness can be measured with the fractal dimension d_f which relates the number of particles N in a floc of size R_f by

$$N=\left(\frac{R_f}{R_0}\right)^{d_f} \tag{1}$$

where R_0 the radius of a primary particle. In the dilute limit, Weitz et al.[14] have shown that $d_f = 1.75$ but the value decreases with increasing concentration to around 1.58 for concentrations above 10^{16} particles per m^3.[15]

An idealized model for the process of diffusion limited aggregation was first described by Smoluchowski in 1917. He modeled the rate of collision between two flocs, containing i and j primary particles, by assuming that (1) the flocs diffuse due to their thermal energy, (2) they are located in an infinite medium, and (3) on collision, they stick irreversibly. If there are n_i flocs containing i primary particles, and r_i is the radius of such a floc, then the expression for the rate of collision is given by[16]

$$J_{ij}=\frac{2kT}{3\mu}\left(r_i+r_j\right)\left(\frac{1}{r_i}+\frac{1}{r_j}\right)n_i n_j \tag{2}$$

Mass conservation requires that the number of flocs of size k increase by aggregation of smaller flocs and decrease as they are consumed upon their own aggregation, hence

$$\frac{dn_k}{dt}=\frac{1}{2}\sum_{i+j=k}J_{ij}-\sum_{i=1}^{\infty}J_{ik} \tag{3}$$

Smoluchowski[16] obtained an analytical solution for Eq. 3 by assuming that the collusion between clusters of similar size dominate, hence

$$\left(r_i+r_j\right)\left(\frac{1}{r_i}+\frac{1}{r_j}\right)=4 \tag{4}$$

With this simplification an expression for the particle distribution can be derived analytically as

$$n_k(t)=n_0\frac{\left(\frac{t}{t_s}\right)^{k-1}}{\left(1+\frac{t}{t_s}\right)^{k+1}} \tag{5}$$

where $t_s=\frac{3\mu}{4n_0kT}$ is called the Smoluchowski time, which is equivalent to the time for half the particles to collide with another and n_0 is the initial number of particles per unit volume, μ the fluid viscosity, and kT the thermal energy.[9]

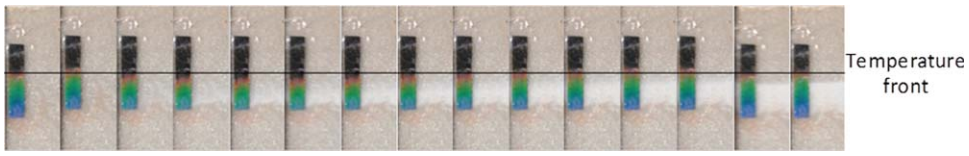

Figure 11. Experiments for the injection of PNIPAM front (7.5 g/L) into a static temperature field, pictures are taken every 5 s, the last two pictures are 60 s apart; (10 cm H_2O head).

The color of the thermochromic strips indicates the temperature. Black indicates a temperature below 30°C, red a temperature above 30°C, green above 31°C, and blue above 35°C. [Color figure can be viewed in the online issue, which is available at wileyonlinelibrary.com.]

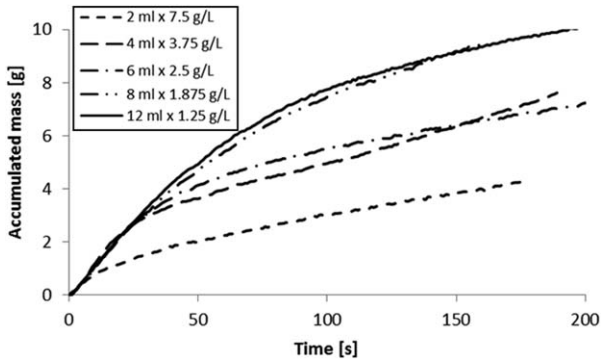

Figure 12. Accumulated mass as a function of time for 0.015 g of PNIPAM injected into a porous bead pack for different volumes of the slug (30 cm H_2O head pressure).

In the present context, as the aggregation proceeds, the model ceases to apply in detail as the confined geometry of the porous matrix impacts Brownian diffusion and the aggregation becomes limited by the geometry of the porous matrix. To estimate the time-scale at which we also expect significant pore blocking, we can match the size of the aggregated flocs with the size of the pore throats, and then compare the number of flocs with the number of pore throats.

We estimate a bead packing fraction of 0.62, and combining this with a measure of the volume of the bead pack, and the size of individual beads, we estimate there are about 9.5×10^9 beads per m^3 in the experimental cell. Sochi and Blunt[17] have shown there are 3.8 beads per pore and 2.8 pore throats per pore, so the number of pore throats in our experiment is about 7.0×10^9 per m^3 in the along flow direction.

Assuming a regular array of spherical beads of diameter D, the pore throat diameter (L_t) and the pore diameter (L_p) can be easily estimated in terms of the bead size as $L_t = L_p - D = D\left(\sqrt{\frac{\pi}{4(1-\varphi)}} - 1\right)$. For the case $D = 0.5$ mm, the pore throat diameter is estimated as 0.115 mm.

The size of primary PNIPAM particles is dependent on the electrolyte concentration and the temperature. Below 32°C the PNIPAM chains are extended. Above 32°C the chains start to collapse on themselves and the effective size becomes smaller. Primary particles are colloidally stable due to charges from initiator moieties located on the chain ends. However, with sufficient salt concentration, the particles form large flocs. The primary particle size was measured in deionized water using dynamic light scattering at 45°C (Brookhaven ZETAPALS) and the results are summarized in Table 1. The effect of polymer concentration on reported size is probably due to a physical crowding effect; extrapolating this data to zero concentration, we estimate a size of around 40 nm for the primary particles.

Various polymer loadings have been used in this work. For simplicity, we estimate a timescale for a polymer loading of 1 g/L. Assuming the primary particles entirely comprise polymer and that the density of PNIPAM is the same as water, the volume fraction of polymer particles may be written as $\frac{4\pi R^3}{3} n_0 = 0.001$, which leads to an initial particle density, n_0, of 3×10^{19} particles per m^3. We can, therefore, estimate the Smoluchowski time as 6 ms. Additionally, the initial loading of 1 g/L equates to 2×10^{21} polymer chains per m^3. This provides the number of polymer chains per primary particle as 67. Using Eq. 5, the time for the number of flocs of size k to equal the number of pore throats is given by $(t/t_s)^{-2} \sim 2.3 \times 10^{-10}$. This time is about 6.5×10^4 times the Smoluchowski time, and corresponds to about 390 s. This compares favorably with Figure 4, where the permeability is seen to plateau when heating is applied for a few hundred seconds.

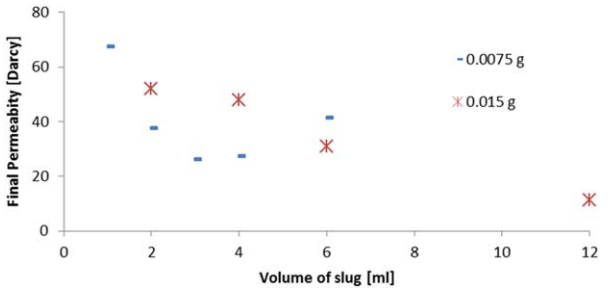

Figure 13. Final permeability as a function of slug volume for various polymer amounts injected into the bead pack.

[Color figure can be viewed in the online issue, which is available at wileyonlinelibrary.com.]

Reduction in Permeability

In this section, we develop a simple two-dimensional pore network model to explore how the permeability of a bead pack evolves if precipitated polymer flocs block a certain proportion of network links. We initially assume the porous medium is homogeneous, and that the polymer flocs are impermeable and hence block the pore-throats; however, we later relax these assumptions and allow for weakly permeable flocs in a heterogeneous pore-throat network. For convenience, we use a pipe network model (EPANET software[18]) modified to account for flow in a porous medium, in which the pressure drop is given by the Hagen–Pouiselle equation

$$\Delta P = \frac{8\mu L Q}{\pi r^4} \tag{6}$$

with Q the volumetric flow rate in the pipe, L the pipe length, and r the pipe radius. Each node is connected to six other nodes through links of the same diameter. Different links in the network were blocked, randomly, to simulate the effect of the precipitation of polymers; for each blocking fraction the model was then run one thousand times to determine the mean and variance of the permeability for each fraction of the network blocked by the permeability. In all calculations, the width of the cell was set to be 1/5th of the along-flow extent of the cell.

The results, in Figure 14, show histograms of one-thousand calculations of the permeability for four different values of the fraction of network links which are assumed to

Table 1. Summary of Hydrodynamic Diameter, Determined by Dynamic Light Scattering

Concentration (g/L)	Diameter (nm)
0.625	45
1.875	62
3.75	67
7.5	86

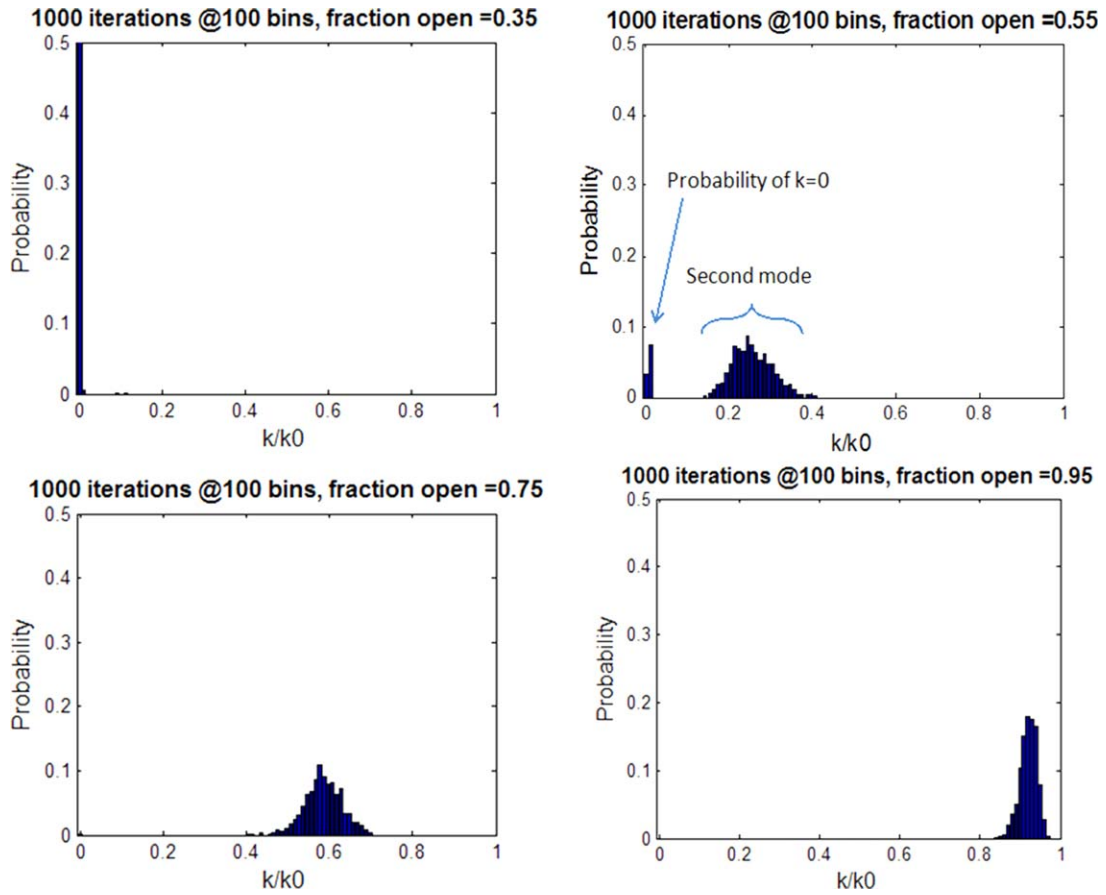

Figure 14. Histograms of bed permeability for various fractions of open channels.

Data created from 1000 independent calculations. [Color figure can be viewed in the online issue, which is available at wileyonlinelibrary.com.]

be blocked. When the fraction of network links blocked in the model is between 0.3 and 0.65, the permeability distribution is bimodal. The lower branch is equivalent to a completely blocked network, whereas the higher branch retains a coherent series of open network links from the upstream to downstream, from which a mean permeability k_{mean} and standard deviation σ can be computed.

Finite Permeability Reduction. We now consider the case where the polymer flocs have a low, nonzero permeability, which is less than the inherent rock permeability. The results are presented in Figure 15 as the average permeability calculated from 1000 simulations. For the case where the polymer had a permeability of 0.5% of the original rock, zero permeability is never achieved, but at very low values for the fraction of pore spaces which remain open, the permeability develops two branches of very low permeability, with the lower one corresponding the case where all flow paths involve flow through a polymer floc. This is shown in Figure 15a. The result can be compared with the case in which the polymer flocs are modeled as being impermeable, as shown in Figure 15b. The bimodal distribution leads to two averages being presented, relating to the entire distribution or alternatively just the nonzero mode.

Log-Normal Pore Size Distribution. We now examine the effect of a distribution of grain sizes, often modeled with a log-normal probability distribution,

$$p(x)=\frac{1}{x\sigma\sqrt{2\pi}}\exp\left(-\frac{(\ln x-\xi)^2}{2\sigma^2}\right) \tag{7}$$

Where $p(x)$ is the probability of a pore throat having a diameter x. The mean of the logarithm of pore throat sizes is ξ and the standard deviation is σ. One thousand iterations were performed for a series of fixed values of the fraction of pore spaces blocked by the polymer flocs, and the effective permeability of the network is recorded. There is a distribution of values for the permeability and as the standard deviation is increased the scatter plots become more dispersed. Figure 16 shows the permeability distribution, for two different standard deviations. As previously seen for the uniform pore size, the permeability distribution becomes bimodal, with some configurations displaying complete blocking.

Discussion

Experimental findings

The time dependence of the permeability reduction as shown in Figure 4 agrees, at least qualitatively, with the time taken for a diffusion limited aggregation of primary PNIPAM particles to form flocs of size comparable to a pore throat. The resultant permeability is affected by polymer concentration, temperature, and salt concentration. This is because of the configuration the polymer chains adopt in different environments and the pore blocking efficiency being affected by the collapse or extension of chains.

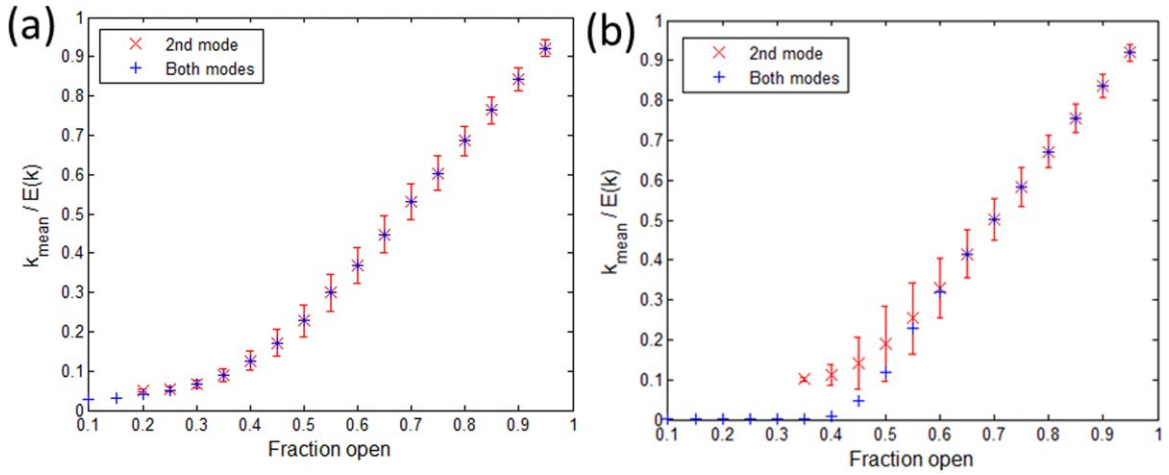

Figure 15. Mean permeability (second mode) and expected permeability *E*(*k*) for the case where (a) the polymer floc has a permeability of 0.5% of the bulk rock and (b) the polymer is impermeable.

[Color figure can be viewed in the online issue, which is available at wileyonlinelibrary.com.]

For high polymer concentrations, the results are insensitive to the initial permeability, as shown in Figure 7. The likelihood is that the polymer flocs have an inherent permeability and this controls the permeability seen at the largest polymer concentrations. Indeed, if the initial bead pack has a permeability, k_0 and the polymer has an effective permeability, k_p, then provided that $\phi k_p << k_o$, the permeability is controlled by the polymer network within the pore spaces, of porosity ϕ.

The precipitation of PNIPAM causes a blockage in the porous media and the drop in permeability. The results in Figure 8 indicate that to cause a blockage in the porous media a critical amount of polymer is required. However, there is no benefit in using any additional polymer. This is quantified by Figure 9, which shows that the bed permeability drops at a certain polymer loading and then flattens. Interestingly lower polymer concentrations allow a lower amount of polymer to be used to block the porous media. This suggests an optimization for polymer floods in the field. The overall view is supported by the photos in Figures 10 and 11, which show an ever thickening precipitated PNIPAM layer, whereas only a thin polymer layer is required to achieve flow blocking.

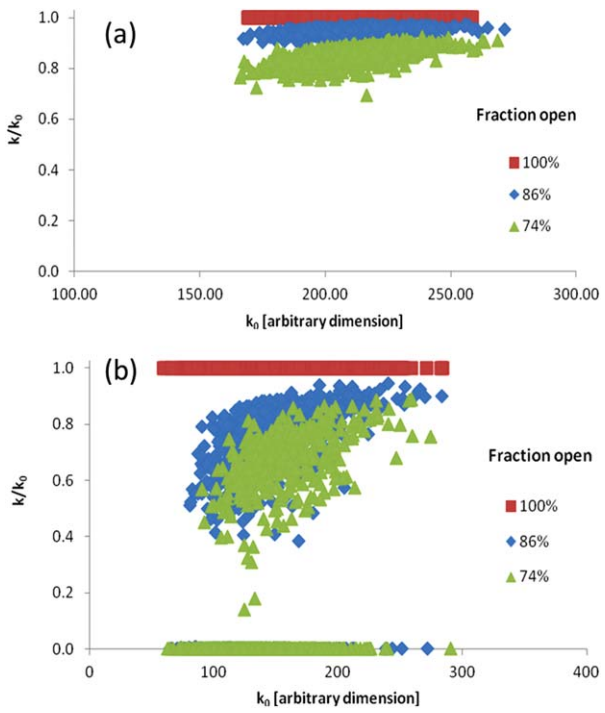

Figure 16. Permeability as a function of initial permeability for 1000 iterations (a) for $\sigma = 0.1$ and (b) $\sigma = 1$.

[Color figure can be viewed in the online issue, which is available at wileyonlinelibrary.com.]

Aggregation model

The model used for aggregation has a number of simplifications albeit explained earlier in the text. It would be interesting to extend the model to account for the suppression of the growth, and of the transport once the flocs become of comparable size to the pores.

The network model was extended to account for heterogeneous pore sizes modeled with a log-normal distribution. Using a probability distribution for different pore throat sizes the permeability of the network can be predicted. As intuitively expected the standard deviation of the pore throat distribution is crucial in determining the breadth of the predicted permeability distribution. The models are valuable in illustrating the complexity of applying the experimental models and results to real applications, in which there will be uncertainty and variability in the response of the system to the polymers.

Conclusions

The temperature sensitive polymer PNIPAM aggregates on heating. When placed in a porous medium the heating and aggregation leads to a reduction in the permeability with the magnitude of the reduction increasing with polymer concentration, temperature, and salinity. The process can be understood, at least qualitatively, by aggregation of polymer particles into flocs that then block pore throats randomly throughout the porous media. The polymer flocs are thought to have a residual permeability and consequently high concentration regions show a more significant reduction in permeability.

Acknowledgments

The authors are grateful to EPSRC for a studentship for ATV and to BP for advice and support.

Literature Cited

1. Lake LW. Enhanced Oil Recovery. Englewood Cliffs, NJ: Prentice Hall, 1991.
2. Sahimi M. Flow phenomena in rocks–from continuum models to fractals, percolation, cellular automata and simulated annealing. *Rev Mod Phys*. 1993;65(4):1393–1534.
3. Tan CT, Homsy GM. Viscous fingering with permeability heterogeneity. *Phys Fluids A*. 1992;4(6):1099–1101.
4. Zimmerman WB, Homsy GM. Viscous fingering in miscible displacements: Unification of effects of viscosity contrast, anisotropic dispersion, and velocity dependence of dispersion on nonlinear finger propagation. *Phys Fluids A*. 1992;4(11):2348–2359.
5. Heskins M, Guillet JE. Solution properties of Poly(N-isopropylacrylamide). *J Macromol Sci Part A*. 1968;2(8):1441–1455.
6. Zhou J, Wang G, Hu J, Lu X, Li J. Temperature, ionic strength and pH induced electrochemical switching of smart polymer interfaces. *Chem Commun*. 2006;46:4820–4822.
7. Pelton RH, Chibante P. Preparation of aqueous lattices with n-isopropylacrylamide. *Colloids Surf*. 1986;20(3):247–256.
8. Morris GE, Vincent B, Snowden MJ. Adsorption of lead ions onto N-isopropylacrylamide and acrylic acid copolymer microgels. *J Colloid Interface Sci*. 1997;190:198–205.
9. Russel W B, Saville DA, Schowalter WR. Colloidal Dispersions. Cambridge: Cambridge University Press, 1991.
10. Hounslow MJ, Ryall RL, Marshall VR. A discretized population balance for nucleation, growth and aggregation. *AIChE J*. 1998;34(11):1821–1832.
11. Lister JD, Smit DJ, Hounslow MJ. Adjustable discretized population balance for growth and aggregation. *AIChE J*. 1995;41(3):591–603.
12. Witten TA, Sander LM. Diffusion limited aggregation, a kinetic critical phenomena. *Phys Rev Lett*. 1981;47(19):1400–1403.
13. Meakin P. Formation of fractal clusters and networks by irreversible diffusion limited aggregation. *Phys Rev Lett*. 1983;51(13):1119–1122.
14. Weitz DA, Huang JS, Lin MY, Sung J. Limits of the fractal dimension for irreversible kinetic aggregation of gold colloids. *Phys Rev Lett*. 1985;54(13):1416–1419.
15. Carpineti M, Ferri F, Giglio M, Paganini E, Perini U. Salt-induced aggregation of polystyrene latex, *Phys Rev A*. 1990;42(12):7347–7354.
16. Smoluchowski MV. Versuch einer mathematischen Theorie der Koagulationskinetik kolloider Losungen. *Z Phys Chem*. 1917;92:129–168.
17. Sochi T, Blunt M. Pore-scale network modeling of Ellis and Herschel–Bulkley fluids. *J Petrol Sci Eng*. 2008;60(2):105–124.
18. United States Environmental Protection Agency (2000) *EPANET 2 USERS MANUAL*, [Online], Available at: http://www.image.unipd.it/salandin/IngAmbientale/Progetto_2/EPANET/EN2manual.pdf. Accessed January 1, 2014.

Manuscript received May 31, 2013, and revision received Sept. 22, 2013.